

Optimal design of high-rise buildings with respect to fundamental eigenfrequency

Arsalan Alavi¹ · Reza Rahgozar¹ · Peyman Torkzadeh¹ · Mohamad Ali Hajabasi²

Received: 21 July 2017 / Accepted: 18 September 2017 / Published online: 25 September 2017
© The Author(s) 2017. This article is an open access publication

Abstract In modern tall and slender structures, dynamic responses are usually the dominant design requirements, instead of strength criteria. Resonance is often a threatening phenomenon for such structures. To avoid this problem, the fundamental eigenfrequency, an eigenfrequency of higher order, should be maximized. An optimization problem with this objective is constructed in this paper and is applied to a high-rise building. Using variational method, the objective function is maximized, contributing to a particular profile for the first mode shape. Based on this preselected profile, a parametric formulation for flexural stiffness is calculated. Due to some near-zero values for stiffness, the obtained formulation will be modified by adding a lower bound constraint. To handle this constraint some new parameters are introduced; thereby allowing for construction of a model relating the unknown parameters. Based on this mathematical model, a design algorithmic procedure is presented. For the sake of convenience, a single-input design graph is presented as well. The main merit of the proposed method, compared to previous researches, is its hand calculation aspect, suitable for parametric studies and sensitivity analysis. As the presented formulations are dimensionless, they are applicable in any dimensional system. Accuracy and practicality of the proposed method is illustrated at the end by applying it to a real-life structure.

Keywords Eigenfrequency · Stiffness distribution · Free vibration · Structural optimization · Tall buildings

Introduction

The optimization subject is of great importance in tall building design that usually requires high material usage. In general, the design process of a tall building involves conceptual design and approximate analysis, preliminary design, and finally detailed design (Jayachandran 2009). Some engineers skip the preliminary design step, in which a proper stiffness distribution is calculated. They usually go straight to the final step after the conceptual design and finalize the structural configuration using some sort of optimization algorithm. However, preliminary design makes it possible to study the problem parametrically. In the review paper done by Aldwaki and Adeli (2014), a vast range of methods proposed by many researchers dealing with tall structures optimization are presented. Almost all of them are code-based and numerical, while a hand calculation method, as in the preliminary design step, is a more suitable tool for sensitivity analyses and parametric studies (Connor and Pouangare 1991).

Although some analytical papers can be found in this field (Kwan 1994; Kaviani et al. 2008; Rahgozar et al. 2010; Malekinejad and Rahgozar 2012), most of them are suitable for abstract analysis but not for design. Moon (2010) introduced a stiffness-based method for optimal design of braced tube systems. For simplicity, shear and flexural resisting systems are assumed to be decoupled with no interaction. The optimal member sizes are determined based on a preselected deformation and observing induced forces. By rather similar approaches, rectangular diagrid tube structures were also studied for optimal stiffness by Moon et al. (2007) and Moon (2012). The problem of polygonal-

✉ Reza Rahgozar
rahgozar@uk.ac.ir

¹ Department of Civil Engineering, Faculty of Engineering, Shahid Bahonar University of Kerman, Kerman, Iran

² Department of Mechanical Engineering, Faculty of Engineering, Shahid Bahonar University of Kerman, Kerman, Iran

section diagrid systems was investigated by Liu and Ma (2017). In the research done by Montuori et al. (2014), strength criteria, in addition to stiffness requirements, is examined in preliminary design of diagrid systems.

Due to more slenderness in new tall structures, controlling the dynamic response is regarded as a serious problem recently. Indeed, motion, rigidity and stability dominate the design requirement instead of strength criteria in such problems. According to Chan et al. (2009), despite of enough lateral resistance against damage to the main structural system of a building, minor damage to nonstructural components or the problem of discomfort to the occupants should be observed. An efficient approach to enhance the dynamic responses of a structure is to optimize its natural frequency. Dynamic behavior of a structure is mainly governed by the fundamental (smallest) natural frequency (Meske et al. 2006; Connor and Laflamme 2014), and maximizing its value, as is done in this research, makes as stiff as possible structure. In this paper, an optimization formulation with the objective of fundamental eigenfrequency is constructed, and it is applied to a cantilever structure, suitable for modeling major motion in a tall building (Connor and Laflamme 2014). It will be shown that the optimality condition is equivalent to enforce the mode shape to have a special format, and stiffness will be calculated based on it. The obtained stiffness is not applicable because of too small values in regions near structure's top; observing a lower bound constraint on stiffness, this problem is resolved. Although such constraints have been explored by many researchers so far, most of them are numerical (Chan et al. 2010; Stromberg et al. 2011; Lee et al. 2012). To deal with this challenging constraint by an analytical approach, the problem is analyzed by introducing a parameter defined as the critical height. In the optimal state, the points above the critical height have the same thickness but different curvature of the first mode profile. Opposite situation exists for thickness and curvature at points lower than the critical height. It will be shown that this strategy makes the problem easy to solve parametrically.

Optimal design of stiffness

Structural modeling

The accepted model for the structure is a one dimensional and continuum cantilever beam, suitable for modeling major motions (Connor and Laflamme 2014), with length ℓ and uniformly distributed mass $m(z) = m$. The bending rigidity $D(z)$ is considered as the only lateral stiffness, as it is approximately true for beam-like structures such as tall buildings (Connor and Laflamme 2014). The coordinate system origin is located at top of the structure (free end)

with positive z direction pointing downward, and the clamped end is located at $z = \ell$.

For the problem of transverse free vibration, if shear deformation, rotary inertia and damping are neglected, the governing differential equation of motion is of the following form (Chopra 2012)

$$m \frac{\partial^2 u}{\partial t^2} + \frac{\partial^2}{\partial z^2} \left[D(z) \frac{\partial^2 u}{\partial z^2} \right] = 0 \quad (1)$$

where $u = u(z, t)$ is in plane transverse displacement in the direction orthogonal to the z axis. Trying a solution of the form $u(z, t) = \phi(z)q(t)$ makes Eq. (1) decoupled into two equations; one for time variable t as

$$\ddot{q}(t) + Aq(t) = 0 \quad (2)$$

and one for spatial variable z as

$$[D(z)\phi''(z)]'' - \Lambda m\phi(z) = 0 \quad (3)$$

where eigenvalue $\Lambda = \omega^2$ is defined for convenience (ω is natural frequency) and will be referred as eigenfrequency. In Eqs. (2) and (3), overdots denote time derivative, and primes denote z derivative, respectively. In related literatures, eigenvector $\phi(z)$ is referred to as mode shape function.

At the clamped end, displacement and slope are both zero; at the free end, bending moment and shear are zero too. Therefore, geometric boundary condition (GBC) is as follows:

$$\text{GBC} \begin{cases} \text{EBC} : \phi(\ell) = \phi'(\ell) = 0 \\ \text{NBC} : [D(z)\phi''(z)]_{z=0} = \left[\frac{d}{dz} [D(z)\phi''(z)] \right]_{z=0} = 0 \end{cases} \quad (4)$$

in which EBC and NBC stands for essential and natural boundary condition, respectively. In the following sections, we deal with governing geometric Eqs. (3) and (4).

Optimization of fundamental eigenfrequency

It is common in optimal design of a dynamic system to maximize fundamental (smallest) eigenvalue $A_f = \omega_{\min}^2$ (Bendsøe and Sigmund 2003; Zheng et al. 2012; Yaghoobi and Hassani 2017) because it mainly dominates the dynamic response of the structure. Therefore, the optimization problem for the accepted model is stated as the following min–max formulation:

$$\begin{cases} \max_{D(z)} \{ A_f = \min A_i, \quad i = 1, \dots, \infty \} \\ \text{s.t.} : \int_0^\ell D(z) dz = U \end{cases} \quad (5)$$

Bending stiffness $[D(z)]$ is selected as the independent variable, and A_f is the smallest eigenfrequency as the objective function. Upper bound U on sum of stiffness is assumed because there is a design constraint on the amount of construction material in any design problem. Otherwise, the optimization problem has no optimal point, because more used material yields more stiffness. According to Rayleigh’s principal, following relation can be used for eigenfrequency A_f and the corresponding eigenvector ϕ_f (Chopra 2012):

$$A_f = \int_0^\ell D\phi_f''^2 dz \tag{6}$$

provided that ϕ_f is normalized to $\int_0^\ell m\phi_f^2 dz = 1$.

Lagrangian method is used here to solve optimization problem (5), so

$$\mathcal{L} = A_f - \lambda \left[\int_0^\ell D(z) dz - U \right] \tag{7}$$

where $\lambda \geq 0$ is the Lagrangian multiplier. Variation of \mathcal{L} with respect to D as the design variable yields

$$\delta\mathcal{L} = \int_0^\ell [(\phi_f''^2 - \lambda)\delta D] dz \tag{8}$$

Optimality condition of $\delta\mathcal{L} = 0$ contributes to the following condition for the eigenvector (mode shape)

$$\phi_f'' = \pm\sqrt{\lambda} = \pm\chi \tag{9}$$

In words, the absolute value of curvature (ϕ_f'') must be constant along the structure at the optimal state. Stiffness will be determined by forcing this objective in the next section.

Optimization of stiffness based on the desired performance

As mentioned before, it is ideal for the mode shape profile to have a uniform curvature characteristic. Considering the positive form of ϕ_f'' in Eq. (9), integrating it twice, enforcing EBC [Eq. (4)] on it, and introducing the dimensionless parameter $\bar{z} = z/\ell$, results to the following:

$$\begin{cases} \phi(\bar{z}) = \chi\ell^2\varphi(\bar{z}) \\ \varphi(\bar{z}) = \frac{1}{2}(\bar{z} - 1)^2 \end{cases} \tag{10}$$

The bending stiffness required to produce a specific profile for the mode shape [Eq. (10)] must be evaluated. To this end, Eq. (3) is considered; ϕ and positive form of ϕ_f'' from Eqs. (10) and (9), respectively, are substituted into Eq. (3) and then integrating it twice observing NBC [Eq. (4)] results to the following relation for stiffness:

$$D(\bar{z}) = \frac{Am\ell^4}{24} (\bar{z}^4 - 4\bar{z}^3 + 6\bar{z}^2) \tag{11}$$

The design constraint presented in optimization problem (5) must be satisfied. Since the dimensionless variable \bar{z} exists in Eq. (11), the mentioned constraint is needed to be restated in variable \bar{z} , as is done in the following:

$$\int_0^1 D(\bar{z}) d\bar{z} = \bar{D} \tag{12}$$

where $\bar{D} = U/\ell$. Equation (12) is named as limited volume constraint because it reflects the limitation of volume of constructional material in practice. Modifying Eq. (11) by multiplying and dividing by \bar{D} and defining a new dimensionless parameter $\theta = \beta\ell$ in which $\beta^4 = Am/\bar{D}$, reduces Eq. (11) to

$$D(\bar{z}) = \frac{\theta^4\bar{D}}{24} (\bar{z}^4 - 4\bar{z}^3 + 6\bar{z}^2) \tag{13}$$

Substituting (13) into constraint (12) dictates that $\theta^4 = 20$. Replacing the obtained value of θ^4 into Eq. (13), the stiffness function can be obtained as

$$D(\bar{z}) = \bar{D}d(\bar{z}) \tag{14}$$

where

$$d(\bar{z}) = \frac{5}{6}\bar{z}^4 - \frac{10}{3}\bar{z}^3 + 5\bar{z}^2 \tag{15}$$

$d(\bar{z})$ is named as the stiffness pattern. The value of $d(\bar{z})$ varies from 0 (for $\bar{z} = 0$) to 2.5 (for $\bar{z} = 1$) by a fourth degree polynomial. The diagram of $d(\bar{z})$ is presented in Fig. 1.

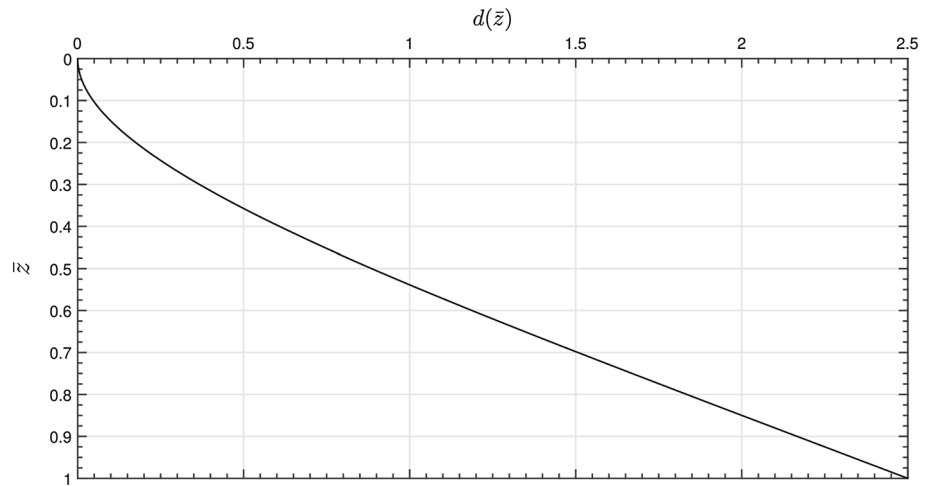
Modified optimization problem (constrained stiffness)

As shown in Fig. 1, the amount of d (and D as the result) approaches zero for the points near top of the structure, which is not right in application. Hence, a lower bound D_{\min} must be observed. That is, D must satisfies $0 \leq D_{\min} \leq D$. Therefore, the new optimization problem would be

$$\begin{cases} \max_{D(\bar{z})} \{A_f = \min A_i, \quad i = 1, \dots, \infty\} \\ \text{s.t. : } \begin{cases} \int_0^\ell D(z) dz = U \\ 0 \leq D_{\min} \leq D \end{cases} \end{cases} \tag{16}$$

In the following sections, some new parameters are defined which simplify treating the new optimization problem (16).

Fig. 1 Stiffness pattern diagram, without a lower bound constraint



Constant stiffness and constant curvature zones

Based on presented diagram in Fig. 1, the lower bound constraint is violated for some points, almost high elevations. It seems helpful to divide the design region into two zones by introducing a specified point as critical height (CH), denoted by \bar{z}_c in dimensionless format. For the points higher than CH ($\bar{z} \in [0 \ \bar{z}_c]$), uniform stiffness D_{\min} with varying curvature of first mode shape is assumed. This region will be called constant stiffness (CS) zone. Inversely, for the points lower than CH ($\bar{z} \in [\bar{z}_c \ 1]$), curvature is constant and the stiffness varies along the height, so it is referred to as constant curvature (CC) zone. Formally, these specifications are as follows; for CS zone

$$CS(0 \leq \bar{z} \leq \bar{z}_c) \begin{cases} \phi''_{CS} = \phi''_{CS}(\bar{z}) \\ D_{CS} = D_{\min} \end{cases} \tag{17}$$

and for CC zone

$$CC(\bar{z}_c \leq \bar{z} \leq 1) \begin{cases} \phi''_{CC} = \chi \\ D_{CC} = D_{CC}(\bar{z}) \end{cases} \tag{18}$$

Mode shape function

The final goal is to determine a parametric formulation for the stiffness. However, the equation of mode shape ϕ is needed for calculating stiffness in prior. Therefore, ϕ is evaluated in different zones at first.

CC zone

The curvature of all points in this region has same value of χ . Considering EBC from Eq. (4) for this region, by a similar way used for (10), results

$$\begin{cases} \phi_{CC}(\bar{z}) = \chi \ell^2 \varphi_{CC}(\bar{z}) \\ \varphi_{CC}(\bar{z}) = \frac{1}{2}(\bar{z} - 1)^2 \end{cases} \tag{19}$$

CS zone

The governing equilibrium Eq. (3) must be solved to determine the mode shape function in CS zone. Substituting the constant stiffness value D_{\min} for $D(z)$ ends in the following governing equation in this zone; in addition GBC is presented:

$$\begin{cases} \phi_{CS}^{IV}(z) - \beta_c^4 \phi_{CS}(z) = 0 \\ \text{NBC} : D_{\min} \phi_{CS}''(0) = \frac{d}{dz} [D_{\min} \phi_{CS}''(z)]_{z=0} = 0 \\ \text{GBC} : \begin{cases} \phi_{CS}(z_c) = \phi_{CC}(z_c) \\ \phi'_{CS}(z_c) = \phi'_{CC}(z_c) \end{cases} \end{cases} \tag{20}$$

where

$$\beta_c^4 = \lambda m / D_{\min} \tag{21}$$

is defined for simplicity. NBC comes from the fact that bending moment and shear are both zero at the free end, and EBC conditions are due to continuity of mode shape function and its derivative in CH point.

The general solution for Eq. (20) is (Chopra 2012)

$$\phi_{CS}(z) = C_1 \sin \beta_c z + C_2 \cos \beta_c z + C_3 \sinh \beta_c z + C_4 \cosh \beta_c z \tag{22}$$

Enforcing NBC on Eq. (22) results in

$$\phi_{CS}(z) = C_1(\sin \beta_c z + \sinh \beta_c z) + C_2(\cos \beta_c z + \cosh \beta_c z) \tag{23}$$

Finally, imposing EBC, Eq. (23) reduces to the following equation for the mode shape in CS zone:

$$\begin{cases} \phi_{CS}(\bar{z}) = \chi \ell^2 \varphi_{CS}(\bar{z}) \\ \varphi_{CS}(\bar{z}) = c \left[\varphi_{CC}(\bar{z}_c) [a_1 f_1(\bar{z}) - a_2 f_2(\bar{z})] + \frac{\varphi'_{CC}(\bar{z}_c)}{\theta_c} [a_1 f_2(\bar{z}) - a_3 f_1(\bar{z})] \right] \end{cases} \quad (24)$$

where

$$\theta_c = \beta_c \ell \quad (25)$$

in which β_c is presented in (21), and $\varphi'_{CC}(\bar{z}_c) = [d\varphi_{CC}/d\bar{z}]_{\bar{z}=\bar{z}_c}$. Other included parameters are defined as

$$\begin{aligned} c &= 1/[2(1 + \cos \theta_c \bar{z}_c \cosh \theta_c \bar{z}_c)] \quad a_1 = \cos \theta_c \bar{z}_c + \cosh \theta_c \bar{z}_c \\ f_1(\bar{z}) &= \cos \theta_c \bar{z} + \cosh \theta_c \bar{z} \quad a_2 = -\sin \theta_c \bar{z}_c + \sinh \theta_c \bar{z}_c \\ f_2(\bar{z}) &= \sin \theta_c \bar{z} + \sinh \theta_c \bar{z} \quad a_3 = \sin \theta_c \bar{z}_c + \sinh \theta_c \bar{z}_c \end{aligned} \quad (26)$$

Optimal distribution of constrained stiffness

Mode shape functions in both CS and CC zones are known from Eqs. (24) and (19), respectively. In addition, the stiffness value in CS zone is known as D_{min} . The stiffness function in CC zone can be determined by use of these knows. To that end, the governing Eq. (3) is integrated twice from 0 to an arbitrary variable $\bar{z} \in [\bar{z}_c, 1]$ (located in CC zone) observing NBC presented in Eq. (4). Integrating region must be divided into two zones of $[0, \bar{z}_c]$ and $[\bar{z}_c, \bar{z}]$, and Eqs. (24) and (19) are used, respectively, for ϕ in each zone. In addition, dimensionless parameter $\bar{z} = z/\ell$ is defined for making relations dimensionless, and χ is substituted for ϕ'' . This calculations result in the following relation for stiffness:

$$D(\bar{z}) = \bar{D} d(\bar{z}) \quad (27)$$

where stiffness pattern $d(\bar{z})$ is written as

$$d(\bar{z}) = \begin{cases} d_{CS}(\bar{z}) = \bar{D}_{min} & 0 \leq \bar{z} \leq \bar{z}_c \\ d_{CC}(\bar{z}) = \bar{D}_{min} \theta_c^4 h(\bar{z}) & \bar{z}_c \leq \bar{z} \leq 1 \end{cases} \quad (28)$$

In which the dimensionless parameter \bar{D}_{min} , with the following relation, is introduced for simplicity:

$$\bar{D}_{min} = \frac{D_{min}}{\bar{D}} \quad (29)$$

and it is named relative minimum stiffness (RMS). $h(\bar{z})$ formulation is as follows,

$$\begin{cases} h(\bar{z}) = g_1 \bar{z} + \int_0^{\bar{z}} g_2(\bar{z}) d\bar{z} \\ g_1 = \int_0^{\bar{z}_c} \varphi_{CS}(\bar{z}) d\bar{z} \quad \text{and} \quad g_2(\bar{z}) = \int_{\bar{z}_c}^{\bar{z}} \varphi_{CC}(\bar{z}) \theta_c d\bar{z} \end{cases} \quad (30)$$

In Eq. (27), \bar{D} shows the amount of used material. Adjusting this parameter, one can control the response of

the structure, such as maximum displacement. However, the stiffness pattern, $d(\bar{z})$, is unchanged.

There are two unknowns \bar{z}_c and θ_c in the presented formulation of $d(\bar{z})$ (h depends on \bar{z}_c and θ_c) to be determined. On the other hand, there are two constraints which must be satisfied; one comes from the continuity of the stiffness, and other is limited volume constraint [Eq. (12)]. These two constraints are observed in the following to evaluate \bar{z}_c and θ_c .

Constraint of continuity of stiffness requires that $D_{CS}(\bar{z} = \bar{z}_c) = D_{CC}(\bar{z} = \bar{z}_c)$, which using Eqs. (27) and (28) results in the following equation:

$$\theta_c^4 h(\bar{z} = \bar{z}_c) - 1 = 0 \quad (31)$$

Equation (31) represents a constraint on \bar{z}_c and θ_c . This equation is solved numerically, and the results are presented in Fig. 2 which presents values of θ_c for different values of $\bar{z}_c \in [0, 1]$. Based on Fig. 2, for $\bar{z}_c = 1$ (uniform stiffness) $\theta_c = 1.8751$; this result is true according to Chopra (2012).

As stated earlier, limited volume constraint must be satisfied. For this end, Eq. (12) is considered; the integration domain $[0, 1]$ is divided into two regions of $[0, \bar{z}_c]$ and $[\bar{z}_c, 1]$, and related formulation of stiffness from Eqs. (27) and (28) are used for each region. The result of integration ends in the following relation

$$\bar{D}_{min} \left(\bar{z}_c + \theta_c^4 \int_{\bar{z}_c}^1 h d\bar{z} \right) - 1 = 0 \quad (32)$$

Satisfying Eq. (31), make θ_c as a function of \bar{z}_c , so there are two unknowns \bar{z}_c and \bar{D}_{min} in Eq. (32). Solving Eq. (32) numerically, one can find the relation between \bar{z}_c and \bar{D}_{min} . Figure 3 presents this relation. Note that D_{min} is always lower than \bar{D} , otherwise the limited volume constraint [Eq. (12)] is violated. Therefore, $\bar{D}_{min} \in [0, 1]$.

At present, all inputs are available to calculate D from Eqs. (27) and (28). In the following, this calculation is summarized by an algorithmic procedure.

Design algorithmic procedure

The design process is summarized here based on before determined information. Going through the following 5-step algorithm, the optimal design will be achieved.

Step 1 [RMS (\bar{D}_{min})]: By use of the design information \bar{D} [Eq. (12)] and D_{min} (a practical constraint), RMS is evaluated from Eq. (29).

Step 2 [CH (\bar{z}_c)]: CH can be determined easily by presented diagram in Fig. 3, using the evaluated RMS from Step 1.

Step 3 [θ_c]: For the known CH from Step 2, θ_c can be determined by use of the presented diagram in Fig. 2.

Fig. 2 Diagram of θ_c versus CH (\bar{z}_c)

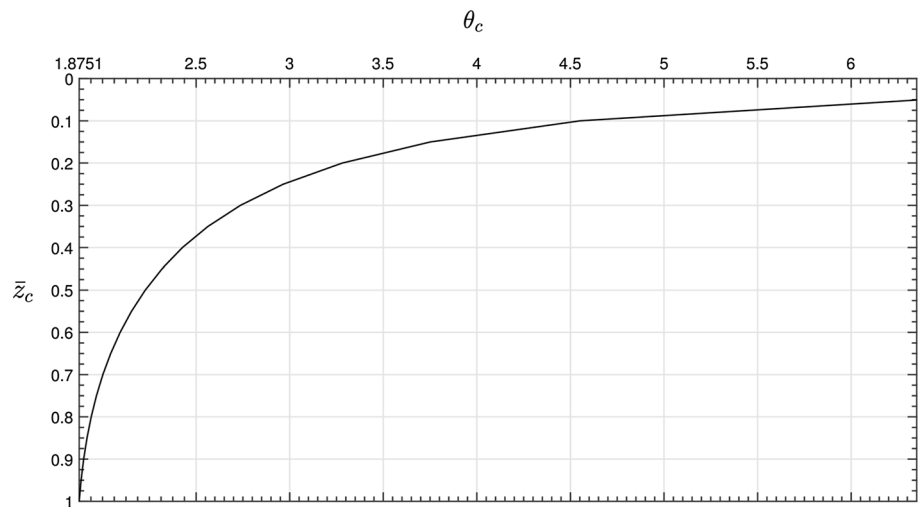
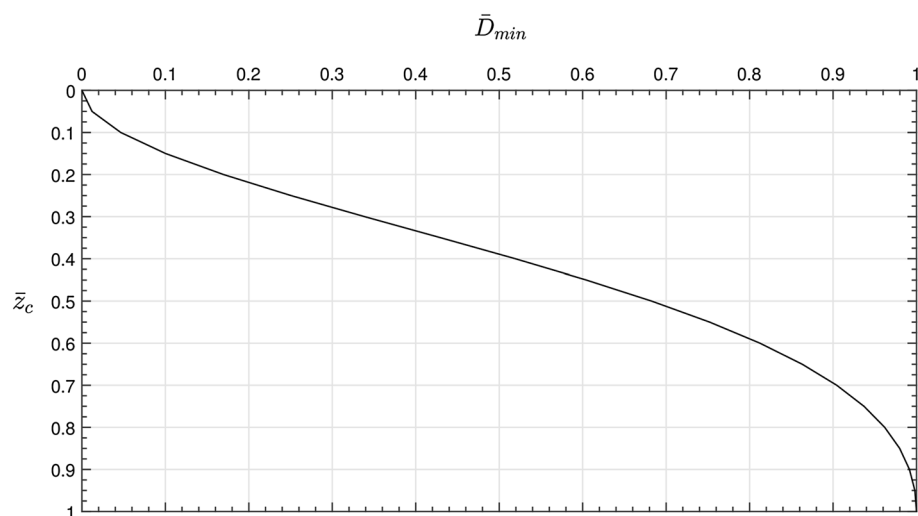


Fig. 3 Diagram of RMS (\bar{D}_{min}) versus CH (\bar{z}_c)



Step 4 [φ]: In this step, φ for each zone is calculated. For CC zone, this function (φ_{CC}) is presented in Eq. (19). Equation (24) presents φ_{CS} , related to CS zone, which needs $\varphi_{CC}(\bar{z} = \bar{z}_c)$, $\varphi'_{CC}(\bar{z} = \bar{z}_c)$, θ_c , \bar{z}_c and presented parameters in (26) as inputs. Therefore, using these parameters φ_{CS} can be determined easily.

Step 5 [optimal stiffness (D)]: By presented formulations in Eqs. (27) and (28), the stiffness function is evaluable. Indeed, using Eq. (28) needs to evaluate h , which in return g_1 and g_2 must be calculated from Eq. (30).

Design graph

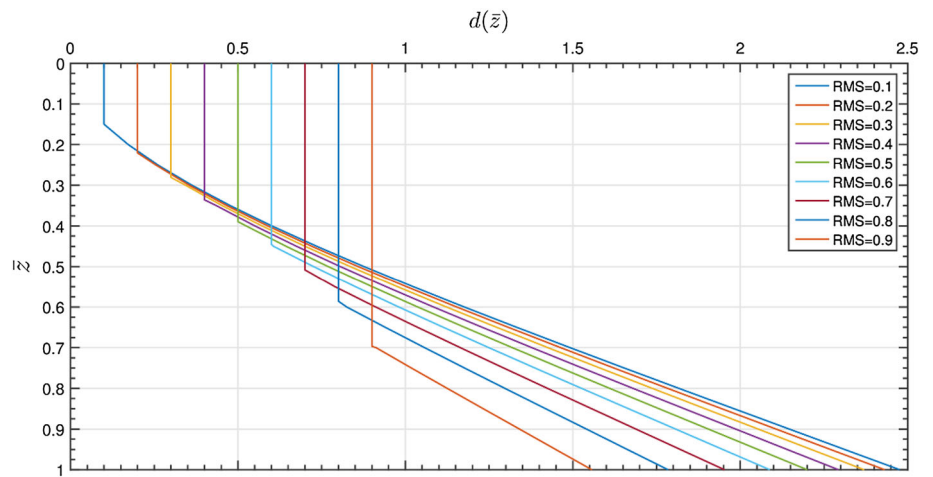
Using the 5-step algorithm includes some equations dealing with may need computer or calculator. As the goal of this paper is to present a hand calculation method for design, the formulation of stiffness pattern [$d(\bar{z})$ in

Eq. (28)] has been evaluated numerically, and its diagram is presented for different values of $\bar{D}_{min} = 0.1, 0.2, \dots, 0.9$, Fig. 4. Constructing new data points within the range of the discrete set of known data points, one can do interpolation. Therefore, knowing RMS (\bar{D}_{min}) as the only input, one can choose the related diagram from Fig. 4. Then, scaling the obtained diagram by \bar{D} [Eq. (27)] yields the value of optimal stiffness.

Illustrative example

This section illustrates the proposed method in application to preliminary design of lateral-resisting systems in tall buildings. Among different systems used in high-rise structures, braced tube is selected here. In this system, the lateral loads are assumed to be carried by exterior frame only; the

Fig. 4 Design graph, for different values of RMS (\bar{D}_{min})



bending strength is generated by closely spaced perimeter columns connected by spandrel beams, and shear forces are resisted by diagonal elements that extended over some stories (Fig. 5). It is assumed that the role of diagonals in bending strength is negligible, as well as the role of perimeter columns in shear resistance (Moon 2010). Therefore, changing dimensions of perimeter columns cannot affect the shearing performance and vice versa. In tall-enough structures, the fundamental eigenfrequency, as the objective function herein, is related to bending. Hence, to optimize this parameter, the perimeter column dimensions are selected as design variable, with the confidence that the shear performance remains unchanged and the fundamental response of the structure is not influenced by it.



Fig. 5 Braced tube system; 780 Third Avenue building

To assess the efficiency of the proposed method, the real-life building known as 780 Third Avenue (Kowalczyk et al. 1995) (Fig. 5) is adapted as the reference point and will be referred to as the basic model in the followings. This structure will be redesigned (with identical amount of material), based on graph of Fig. 4, as the proposed model. Two models are then analyzed, and the results will be compared at the end. The mentioned building is a concrete tube system, braced by shear walls in a cross and zigzag pattern in wide and narrow faces, respectively (Fig. 8). The geometrical information of this building is presented in Table 1 (Kowalczyk et al. 1995).

Structural modeling and definitions

As mentioned above, shear and bending resisting systems can be decoupled into two separate systems. Closely spaced columns located on structure’s perimeter increase effective moment of inertia to resist the bending moments. Hence, a cantilevered box beam, Fig. 6, is a reasonable model for the bending system (Smith and Coull 1996).

In the presented model in Fig. 6, thickness of the box, t , accounts for the perimeter columns and is taken as the only independent variable. As the relations in this paper are constructed based on stiffness (D), it would be beneficial to present D as a function of thickness (t), so

$$D(\bar{z}) = (EI_0) t(\bar{z}) \tag{33}$$

where E is the Young’s modulus of elasticity and $I_0 = [(4/3)b^3 + 4ab^2]$, in which $2a = 38.12$ m and $2b = 21.08$ m are perimeter dimensions based on Fig. 6 that their values are presented in Table 1.

In addition, we need a relation to calculate the dimensions of columns from the thickness (t). According to the relation presented by Kwan (1994), thickness of the box can be calculated as

Table 1 780 Third Avenue geometrical information

Floors above ground	Typical story height	First story height	Structural height	Plan dimensions	Column spacing
49	3.5 m	4.4 m	172.4 m	38.12 m × 21.08 m	2.84 m

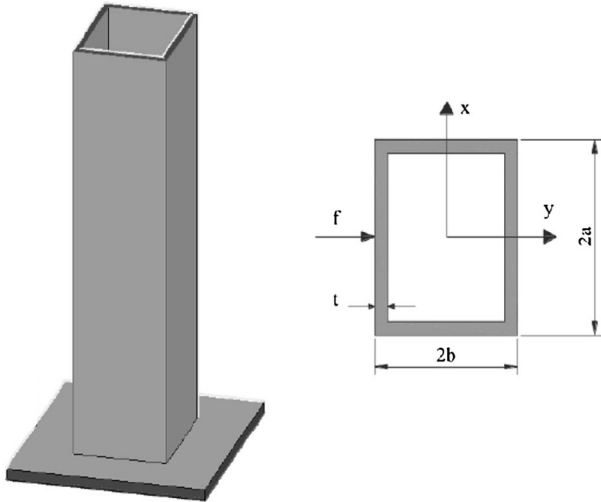


Fig. 6 Beam model with hollow box section for bending resisting system of the structure

$$t = A_c / s \tag{34}$$

in which t is same as used in Eq. (33), A_c is the sectional area of the columns, and s is the columns' spacing which is 2.84 m here (Table 1). In basic structure, perimeter columns are 1.2 m wide, and depth reduces from 0.457 to 0.406 to 0.356 m at floors 19 and 31 (Kowalczyk et al. 1995), Fig. 7a. Thus, the design domain of basic structure

consists of three zones, each of which has uniform column area (A_c).

Structural design

The only needed information to use design graph presented in Fig. 4 is RMS (\bar{D}_{min}) which in turn needs two more inputs \bar{D} and D_{min} , based on Eq. (29). Substituting Eq. (33) into Eq. (12), we have the following relation for \bar{D} :

$$\begin{aligned} \bar{D} &= \int_0^1 (EI_0) t d(\bar{z}) = \int_0^{0.385} (EI_0)(0.1504) d(\bar{z}) \\ &+ \int_{0.385}^{0.63} (EI_0) (0.1715) d(\bar{z}) \\ &+ \int_{0.63}^1 (EI_0) (0.1931) d(\bar{z}) = (EI_0)(\bar{t}) \end{aligned} \tag{35}$$

where

$$\bar{t} = 0.1714 \tag{36}$$

Integration limits are non-dimensional and related to zone limits of basic model. Thickness (t) of each zone can be calculated using Eq. (34). Considering Eq. (33), the following relation can be written for D_{min} :

$$D_{min} = (EI_0) t_{min} \tag{37}$$

where t_{min} is a design constraint which could be dependent on some practical requirements. Suppose minimum depth

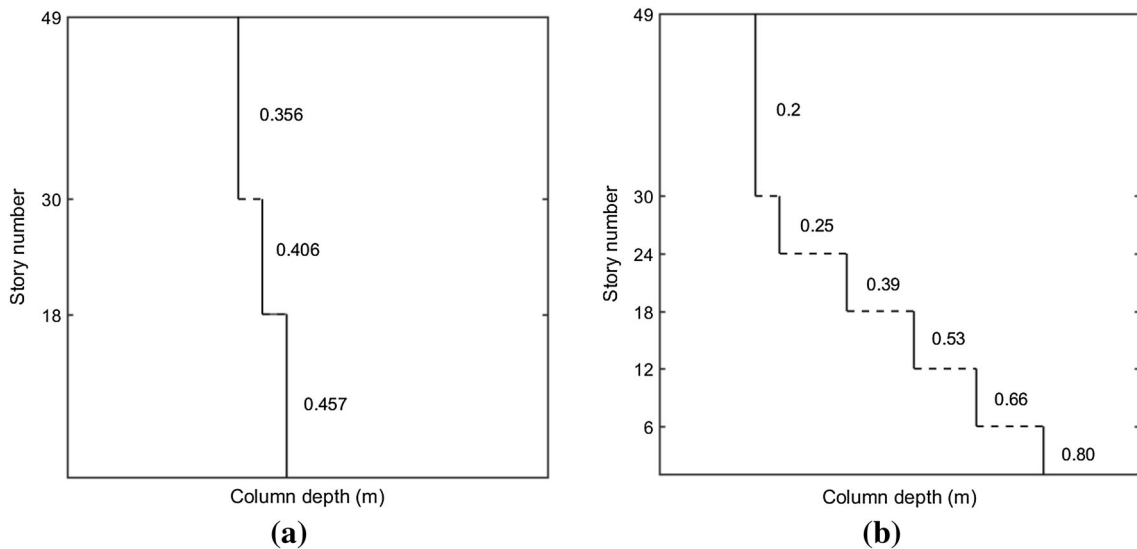


Fig. 7 Design graph of example **a** basic structure, **b** proposed structure

of 0.2 m for columns and keep their width unchanged (1.2 m). Thus, the minimum sectional area would be 0.24 m^2 , so using Eq. (34) for $s = 2.84 \text{ m}$, we have

$$t_{\min} = 0.0845 \text{ m} \quad (38)$$

as the minimum thickness of the box. Therefore, based on Eqs. (29), (35) and (37), and using the obtained values for \bar{t} and t_{\min} from Eqs. (36) and (38), respectively,

$$\bar{D}_{\min} = \frac{t_{\min}}{\bar{t}} = 0.4929 \quad (39)$$

Referring to Fig. 4 and choosing $\text{RMS} = 0.5$ (approximate value instead of 0.4929), the related diagram for stiffness pattern [$d(\bar{z})$] is selected (the green one). Based on this diagram, CH is 0.386 in its dimensionless format. Using total height of 172.4 m (Table 1), its dimensional value is 66.4 m. Dividing 66.4 m by 3.5 m (typical story height), results approximately 19 stories as the CS zone. Thus, the last 19 stories of the proposed model must have minimum value of stiffness. For the other stories, $d(\bar{z})$ can be determined from the selected diagram. However, as the value of $d(\bar{z})$ varies continuously and is not practical, the design domain must be divided into some zones with constant value of $d(\bar{z})$. Based on Fig. 8b, each diagonal element ties six stories. It seems reasonable to choose every 6 stories as a zone. Therefore, typical length of each zone is about 21 m with non-dimensional value of 0.1218 (0.1270 for the first zone containing first floor). Thus, each zone limits elevation can be determined, and the related value of $d(\bar{z})$ can be read from the selected graph. For example, the first zone of proposed structure concludes story 1–6 with elevation span from 150.5 to 172.4 m. The dimensionless values of the span limits are 0.873 and 1 with value of $d(\bar{z})$ as 1.81 and 2.2, respectively, based on

the selected graph. The limitation that must be observed while calculating a constant value for $d(\bar{z})$ in each span is to keep the material volume unchanged. For simplicity, it is assumed that $d(\bar{z})$ varies linearly in each span. Thus, 2, as the average of 1.81 and 2.2, is selected for the constant value of stiffness pattern (d) in this zone.

To calculate equivalent thickness from the obtained value of d in the previous part, Eqs. (27), (33) and (35) are used which results in

$$t = \bar{t} d \quad (40)$$

By use of the value of \bar{t} from Eq. (36) into Eq. (40), equivalent thickness of each zone is calculated. Considering first zone as example, substituting 2 as d in (40) yields $t = 0.3428$. All that remains is to evaluate the sectional area of columns based on equivalent thickness t . Substituting the obtained t into Eq. (34), with $s = 2.84 \text{ m}$, columns' sectional areas are determined. Supposing uniform width of 1.2 m for columns, their depth can be simply calculated using the sectional area values. This calculation yields 0.8 m for the first zone. Other zones information can be found from Fig. 7.

Software analysis and results

In previous part, the optimal dimensions of the columns are obtained by a hand calculation and simple approach. To evaluate enhancement of the proposed structure compared to basic one, both of them are analyzed in SAP2000 (2013). To construct models in the software, geometrical information from Table 1 and column dimensions presented in Fig. 7 are used. The bracing pattern is presented in Fig. 8, and the thickness of filled panels in basic model is the same as adjacent columns. The bracing geometry in proposed model is completely similar to that of basic one to assess just bending system role in dynamic response. The effective mass is about 800 kg/m^2 , and compressive strength of concrete is about 35 MPa.

The modal analysis outputs show that the fundamental period of the new structure is 4.26 versus 4.77 s related to basic model. That means, fundamental eigenfrequency as the objective function is improved in the proposed structure to some extent. This fact shows that, in addition to simplicity of the proposed method, the result is satisfactory in application.

Conclusions

Due to importance of dynamic responses in design of high-rise structures, vibrational characteristics are investigated. An optimization problem with the objective of fundamental eigenfrequency, the main effective factor in dynamic

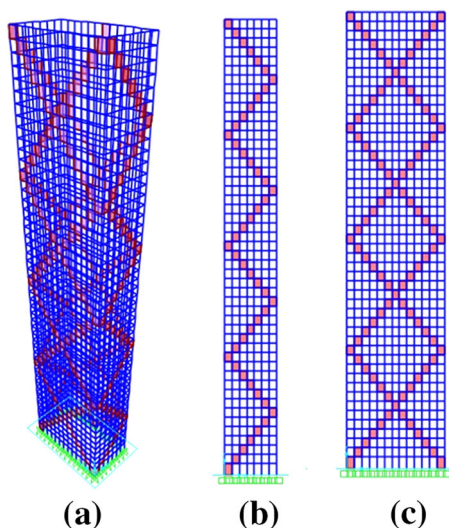


Fig. 8 Model used in SAP2000 **a** 3D, **b** narrow face, **c** wide face

response, is constructed. Flexural stiffness is selected as the only independent variable and its optimal value is calculated. Some major results are as follows,

- Applying calculus of variation on the optimization problem contributes to a specific profile for the first mode shape as the optimality condition. The stiffness, required to produce this profile for the mode shape, is evaluated.
- The optimization problem is modified then by adding the practical constraint of lower bound on stiffness. To treat this new optimization problem by an analytic strategy, new parameters CH, CC and CS were introduced to construct the parametric model. In assessing the effect of design constraints, non-dimensional parameter, RMS, was introduced also.
- The resulting mathematical model yielded diagrams, relating unknown parameters. Based on these diagrams, a simple algorithmic procedure for design is presented.
- To make the design procedure more convenient in practice, the problem of optimal design has been solved for almost all possible values of RMS (0.1, ..., 0.9) and presented as a design graph.
- Accuracy and simplicity of the method were demonstrated by applying it to a real-life structure, which was redesigned utilizing the proposed method. Modal analyses show an 11% enhancement in structural response as compared to that of the original structure; thereby validating the method as a fast and reliable approach in design process of tall buildings.
- The closed-form solutions and presented graphs may serve as benchmarks for numerical studies in optimal design of 2- or 3-dimensional models and for basic understanding.

Open Access This article is distributed under the terms of the Creative Commons Attribution 4.0 International License (<http://creativecommons.org/licenses/by/4.0/>), which permits unrestricted use, distribution, and reproduction in any medium, provided you give appropriate credit to the original author(s) and the source, provide a link to the Creative Commons license, and indicate if changes were made.

References

- Aldwaki M, Adeli H (2014) Advances in optimization of highrise building structures. *Struct Multidiscipl Optim* 50(6):899–919
- Bendsøe MP, Sigmund O (2003) *Topology optimization: theory, methods and applications*. Springer, Berlin, Heidelberg, New York
- Chan C, Huang M, Kwok K (2009) Stiffness optimization for wind-induced dynamic serviceability design of tall buildings. *J Struct Eng* 135(8):985–997
- Chan C, Huang M, Kwok K (2010) Integrated wind load analysis and stiffness optimization of tall buildings with 3D modes. *Eng Struct* 32(5):1252–1261

- Chopra AK (2012) *Dynamics of structures, theory and applications to earthquake engineering*. Pearson Education, Prentice Hall, Upper Saddle River
- Connor J, Laflamme S (2014) *Structural motion engineering*. Springer International Publishing, Basel
- Connor J, Pouangare C (1991) Simple model for design of framed-tube structures. *J Struct Eng* 117(12):3623–3644
- Jayachandran P (2009) Keynote lecture. In: *International conference on tall buildings and industrial structures*
- Kaviani P, Rahgozar R, Saffari H (2008) Approximate analysis of tall buildings using sandwich beam models with variable cross-section. *Struct Des Tall Spec Build* 17(2):401–418
- Kowalczyk RM, Sinn RS, Kilmister MB (1995) *Structural systems for tall buildings*. McGraw-Hill Inc, New York
- Kwan A (1994) Simple method for approximate analysis of framed tube structures. *J Struct Eng* 120(4):1221–1239
- Lee S, Bobby S, Spence S, Tovar A, Kareem A (2012) Shape and topology sculpting of tall buildings under aerodynamic loads. In: *20th analysis and computation specialty Conference*
- Liu C, Ma K (2017) Calculation model of the lateral stiffness of high-rise diagrid tube structures based on the modular method. *Struct Des Tall Spec Build* 26(4):e1333
- Malekinejad M, Rahgozar R (2012) A simple analytic method for computing the natural frequencies and mode shapes of tall buildings. *Appl Math Model* 36(8):3419–3432
- Meske R, Lauber B, Schanck E (2006) A new optimality criteria method for shape optimization of natural frequency problems. *Struct Multidiscipl Optim* 31(4):295–310
- Montuori GM, Mele E, Brandonisio G, Luca AD (2014) Design criteria for diagrid tall buildings: stiffness versus strength. *Struct Des Tall Spec Build* 23(17):1294–1314
- Moon KS (2010) Stiffness-based design methodology for steel braced tube structures: a sustainable approach. *Eng Struct* 32(10):3163–3170
- Moon KS (2012) Optimal configuration of structural systems for tall buildings. In: *20th analysis and computation specialty conference*
- Moon KS, Connor J, Fernandez JE (2007) Diagrid structural systems for tall buildings: characteristics and methodology for preliminary design. *Struct Des Tall Spec Build* 16(2):205–230
- Rahgozar R, Ahmadi A, Sharifi Y (2010) A simple mathematical model for approximate analysis of tall buildings. *Appl Math Model* 34(9):2437–2451
- SAP2000 (2013) *Ultimate 16.0.0, Structural Analysis Program*, Computer and Structures Inc., Berkeley, USA
- Smith S, Coull A (1996) *Tall building structures*. McGraw Hill Book Company, New York
- Stromberg LL, Beghini A, Baker WF, Paulino G (2011) Application of layout and topology optimization using pattern gradation for the conceptual design of buildings. *Struct Multidiscipl Optim* 43(2):165–180
- Yaghoobi N, Hassani B (2017) Topological optimization of vibrating continuum structures for optimal natural eigenfrequency. *Int J Optim Civ Eng* 7(1):1–12
- Zheng J, Long S, Li G (2012) Topology optimization of free vibrating continuum structures based on the element free Galerkin method. *Struct Multidiscipl Optim* 45(1):119–127

Publisher's Note

Springer Nature remains neutral with regard to jurisdictional claims in published maps and institutional affiliations.

